Coulombic Efficiency for Practical Zinc Metal Batteries: Critical Analysis and Perspectives

(article starts on next page)

Coulombic Efficiency for Practical Zinc Metal Batteries: Critical Analysis and Perspectives

Zhenrui Wu, Yihu Li, and Jian Liu*

Climate change and energy depletion are common worries of this century. During the global clean energy transition, aqueous zinc metal batteries (AZMBs) are expected to meet societal needs due to their large-scale energy storage capability with earth-abundant, non-flammable, and economical chemistries. However, the poor reversibility of Zn poses a severe challenge to AZMB implementation. Coulombic efficiency (CE) is a quantitative index of electrode reversibility in rechargeable batteries but is not well understood in AZMBs. Thus, in this work, the state-of-art CE to present the status quo of AZMB development is summarized. A fictional 120 Wh kg^{-1} AZMB pouch cell is also proposed and evaluated revealing the improvement room and technical goal of AZMB chemistry. Despite some shared mechanisms between AZMBs and lithium metal batteries, misconceptions prevalent in AZMBs are clarified. Essentially, AZMB has its own niche in the market with unique merits and demerits. By incorporating academic and industrial insights, the development pathways of AZMB are suggested.

1. Introduction

Aqueous zinc metal battery (AZMB) is a rechargeable battery chemistry built by an aqueous electrolyte, a Zn metal or alloy anode, and usually a Zn-free cathode such as MnO_2 and V_2O_5. In diluted aqueous electrolytes, a $[Zn(H_2O)_6]^{2+}$-based solvation structure is present due to the strong polarity of water molecules.[1] Zn metal is the main body of the AZMB anode that achieves reversible energy storage via a Zn^{2+}/Zn redox pair of Zn plating and stripping. Because of the substantial water reactivity with Zn, side reactions of Zn corrosion (in acid), Zn passivation (in base), and

Z. Wu, J. Liu
School of Engineering
Faculty of Applied Science
The University of British Columbia
Kelowna V1V 1V7, Canada
E-mail: jian.liu@ubc.ca
Y. Li
Department of Physics
Chalmers University of Technology
Göteborg SE-41296, Sweden

The ORCID identification number(s) for the author(s) of this article can be found under https://doi.org/10.1002/smtd.202300660

hydrogen (H_2) evolution are prevalent.[2] Very recently, Zhu et al. reported an underpotential deposition (UPD) of Zn at the cathode at 0.3 V versus Zn^{2+}/Zn, another Zn-irreversibility-related capacity decay mechanism.[3]

The main salt of AZMB electrolyte is Zn salt, such as $ZnSO_4$, $Zn(SO_3CF_3)_2$, $Zn(TFSI)_2$, etc. Cation additives can regulate Zn electrodeposition via solid electrolyte interphase (SEI) formation,[4] heteroatom doping,[5] in situ alloying,[6] electrostatic shielding,[7] electric double layer (EDL) repulsion,[8] etc. Functional anions (e.g., ClO_4^-,[9] Cl^-)[10] and molecular additives (e.g., NMP,[11] TMP,[12] methanol)[13] are expected to change the solvation sheath structure of Zn^{2+}, enhancing the electrolyte performance in extending the electrochemical stability window (ESW) or thermal stability window (TSW) and forming a functional SEI, and adjust Zn^{2+} kinetics, ameliorating the dendritic growth of Zn.[14] Studies have reported effective cation-anion synergetic strategies in enhancing the overall AZMB performance.[15] The anion effect in polymer electrode cycling stability has also been explored.[16]

In addition to anode and electrolyte, high-performance cathode materials such as MnO_2, V_2O_5, Prussian blue analogs (PBAs), and NASICON-type polyanions (PAs) are developed and studied intensively.[17] The Zn^{2+} storage mechanism in each cathode varies. Transitional metal dichalcogenides, PBAs, and layer-structured transitional metal oxides (TMOs) can show an H^+/Zn^{2+} co-insertion in mildly acidic AZMB,[18] providing competent capacity to the battery; the small size and fast mobility of H^+ also benefit a structurally stable cathode material.[19] Chuai et al. constructed a 1.95-V AZMB via the dissolution mechanism of the MnO_2/Mn^{2+} pair.[20] PAs with proper electrolytes can show a dual-cation insertion, such as Na^+/Zn^{2+} or Ca^{2+}/Zn^{2+} co-insertion in $Na_3V_2(PO_4)_3$.[21] The conversion mechanism applies to some TMOs (e.g., Co_3O_4)[22] and traditional conversion-type cathodes (e.g., I_2, Br_2; S, Se, Te).[23] Non-metallic anions (e.g., OH^-, Cl^-) can act as charge carriers, too.[24] However, battery chemistry built from these anions can show a severe self-discharging effect for redox pairs containing a soluble oxidation product, such as Br^-/Br_3^- and I^-/I_3^-.[25] Organic cathode achieves charge transfer via an ion-coordination mechanism of radical anions.[26]

Despite the variety of cathodic half-reactions, the charge carrier and redox center of the anode in AZMBs are Zn ions, and
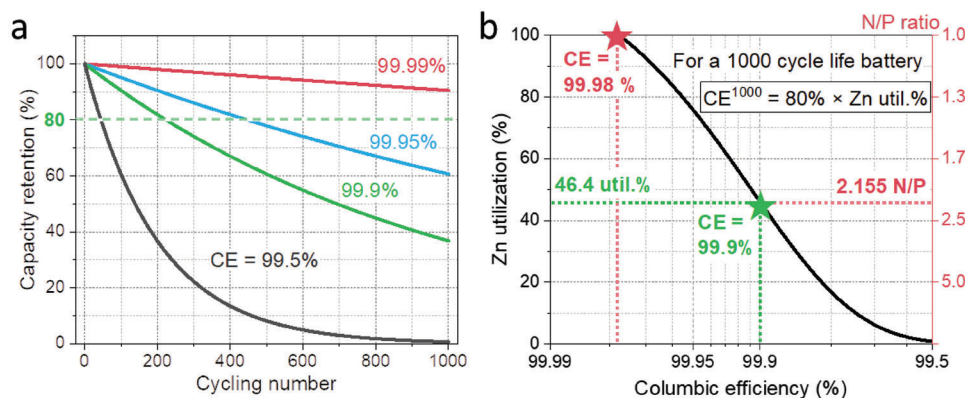
Figure 1. a) Capacity retention at varied CEs and b) required CE by cycle life.

the Zn^{2+}/Zn reversibility is intrinsically problematic and becomes the main limitation of the overall Coulombic efficiency of AZMBs. In this work, we summarize the state-of-the-art CE of Zn stripping and plating in AZMBs and offer perspectives on CE improvement strategies. More importantly, learning from lithium metal battery (LMB) and lithium-ion battery (LIB) development history, we propose a fictional 120 Wh kg^{-1} AZMB pouch cell configuration and suggest a three-stage energy density boosting trajectory.

2. Significance of CE

2.1. CE Dictates Zn Reversibility

CE quantitatively describes the redox reversibility of rechargeable batteries. However, in AZMB studies, the significance of CE has been overlooked. Studies on the Zn metal anode and Zn electrodeposition regime often use Ti/Zn asymmetric cells to avoid the disturbance from the cathode issues. In the Ti/Zn configuration, CE represents the reversibility of Zn stripping and plating on the Ti metal substrate. A homogeneous Zn deposition is essential to achieve high reversibility of AZMBs because a preferential deposition leads to varied areal capacity at different locations, uneven utilization of the cathode, and, thus, severe capacity loss in a full battery.[27] Considering the cathode's dissolution and instability issue and water's high activity in an aqueous electrolyte, the capacity loss can collectively result from multiple side reactions.

The irreversible capacity can originate from two main factors:

1) *Parasitic Reactions at the Electrode-electrolyte Interface*: H$_2$ gas emission has been observed during Zn plating,[28] dissolvable by-products are possible, and the passivation behavior of Zn is widely known.[29] These side reactions do not contribute to reversible Zn^{2+} storage but produce an irreversible capacity that can be reflected in a cyclic voltammetry (CV) test. These reactions occur only in the first few cycles until an SEI is formulated and functioning.

2) *Capacity Loss of Active Materials*: This occurs gradually throughout the life cycle of a battery. The sources include cathode dissolution, structural decay in charge and discharge cy-

cles, "dead" Zn detached from dendrites, etc. Compared with the cathodic Zn intercalation/deintercalation, the anodic Zn stripping/plating is considered a limitation of the overall reversibility of a battery due to the natural dendritic growth of Zn that can abruptly trigger a short-circuit dysfunction.

2.2. CE Tells Battery Life Cycle

The capacity retention ratio of a rechargeable battery is the retained capacity (Q_n) of a particular cycle number (n) out of the initial capacity (Q_0) in percentage (Equation 1).[30] The cycle life of a battery is the total cycle number (n) completed when the retention ratio drops to 80%. As shown in **Figure 1**a, a long-cycle-life battery needs a consistently high CE. A poor CE leads to exponential capacity decay. Only with a nearly unattainable CE of >99.98% can the battery achieve a 1000-cycle life with 80% capacity retention (Figure S1, Supporting Information).

$$\text{capacity retention ratio} = \frac{Q_n}{Q_0} \times 100\% = CE^n \ (= 80\%) \tag{1}$$

It is worth mentioning that a high average CE does not necessarily guarantee a long cycle life of batteries.[27] In addition to the gradual capacity loss of Zn and cathode material, the battery can suddenly become dysfunctional due to some abrupt causes despite a sufficient Zn reservoir, such as electrolyte depletion (open circuit due to ion immobility), H$_2$ evolution (irreversible capacity, local pH change) and accumulation at the interface (open circuit), or dendrite formation (short circuit).[31] These triggers are prevalently existing yet unpredictable by standard electrochemical methods.

2.3. Relate CE to Battery Design

However, full batteries are formulated with a negative-to-positive capacity ratio (N/P), which quantitatively describes the excessive anode capacity versus the cathode capacity (Equation 2). In AZMB chemistry, it means a more active Zn reservoir. Lab-scale AZMB studies use excessive Zn metal at the anode to compensate for the poor CE. Since active Zn is dominantly from the Zn

metal anode in AZMBs, researchers use another equivalent concept, Zn utilization percentage (Zn util.%), to present the actual areal capacity of Zn being charged and discharged versus the total anode capacity loading in AZMBs (Equation 3). Referring to the state-of-the-art LMB pouch cells N/P of 2, for Zn chemistry, Figure 1b indicates that when Zn util.% = 46.4% (N/P = 2.155), the required CE of a 1000-cycle-life battery can be relaxed from 99.98% to 99.9%. This controlled Zn excess makes an ultra-stable AZMB an achievable goal.

$$N/P = \frac{Zn\ anode\ capacity}{Cathode\ capacity} \quad (2)$$

$$Zn\ util.\% = \frac{Actual\ areal\ capacity}{Zn\ anode\ capacity} \times 100\% \quad (3)$$

3. Critical Analysis on a Pouch-cell Basis

3.1. Feasibility of a 120 Wh kg⁻¹ AZMB Pouch Cell

The high performance of a secondary battery comes from two indices: competent energy density and good cycling stability. On the one hand, the practical energy density of a pouch cell is often much smaller than the theoretical energy density of the active materials because multiple inactive components, such as binders, conductive additives, electrode porosity, electrolytes, separators, and packing materials, do not contribute to the capacity. Technically, the smaller N/P or E/C, the merrier the energy density. To be more exact, the maximum gravimetric energy density (E_m) a MnO_2/Zn pouch cell can realize (232 Wh kg⁻¹) is calculated to be 58% of the material-level E_m of MnO_2 (400 Wh kg⁻¹). The calculation method is provided in the Supporting Information (chapter 1). On the other hand, AZMBs have a lot of improvement room in their cycling stability, where their anode incapability worries the most. Due to the instability Zn-H_2O interface, expecting an N/P = ≈1 like LIBs is unrealistic.

The conundrum is that a high N/P providing extra Zn reservoir can compensate for the inferior CE of Zn reversibility, enhancing the battery cycling stability but, at the same time, decreasing the nominal energy density of the battery. By analyzing the present studies of AZMBs and the development pathway of LIBs and LMBs, we figured that developing a high-performance 120 Wh kg⁻¹ AZMB pouch cell is a challenging but achievable goal only with MnO_2 among all present cathodes with decent reversibility. An N/P = 2.155 could reduce the CE requirement of Zn metal reversibility from 99.98% (nearly unrealizable) to 99.9% (challenging but achievable), aiming for a 1000-cycle rechargeable battery. The technical parameters are summarized in **Table 1**. In addition to the low cost and safety benefits, the attainable high energy density makes AZMB an excellent candidate for stationary large-scale energy storage.

The mass loading determination needs to consider the active materials' mechanical and electrochemical properties. A recent study demonstrated a 1 Ah and 70 Wh L⁻¹ $Zn_{0.25}V_2O_5$/Zn 2-layer pouch cell with a 5.5 mAh cm⁻² loading and an N/P = 3.2.[33] Recent studies on LMBs underline that next-generation 500 Wh kg⁻¹ LMBs must elevate the capacity loading to 6–7 mAh cm⁻².[34] Due to the similar chemistry of AZMB and commercial LMB

Table 1. Technical parameters of a fictional 120 Wh kg⁻¹ MnO_2/Zn pouch cell.

Cell Component	Cell Parameters	Value
MnO_2 Cathode	Reversible capacity (mAh g⁻¹)	308[32]
	Unilateral active material loading (mg cm⁻²)	22
	Unilateral areal capacity (mAh cm⁻²)	6.78
	Active material weight ratio	96%
	Electrode press density (g cm⁻³) / porosity	3.7 / 25%
	Unilateral electrode thickness (μm)	65
	Electrode length × width (mm)	70 × 40
	Unilateral Ti foil thickness (μm)	5
	Number of cathode sheets	16
Zn Anode	N/P capacity ratio	2.155
	Unilateral Zn foil thickness (μm)	25
Electrolyte	E/C ratio (g Ah⁻¹)	3
	Areal weight (mg cm⁻²)	20
Separator	Thickness (um)	50
Packing Materials	Al laminated film thickness (μm)	115
	Ni tab dimensions (mm)	25 × 8 × 0.02
	Insulating mat dimensions (mm)	10 × 10 × 0.02
Pouch Cell	Capacity (Ah)	3
	Operating voltage (V)	1.3
	Gravimetric energy density (Wh kg⁻¹)	120
	Volumetric energy density (Wh L⁻¹)	550

cathode (both are transitional metal oxides), the same loading (22 mg cm⁻²) should be benchmarked for AZMBs, which gives a capacity loading of 6.78 mAh cm⁻². A 25-μm Zn foil is needed to match this loading (N/P = 2.155). Given that the thinnest Zn foil of 10 μm is already circulating in the market, the leading technology bottleneck for a small enough N/P ratio still lies in the lousy CE. Other assumptions in Table 1 are provided in Table S1, Supporting Information. A detailed calculation method is written in the Supporting Information.

Figure 2a–c illustrate the composition of a fictional 3-Ah and 120 Wh kg⁻¹ AZMB pouch cell. It is worth noting that even with such a constrained N/P ratio of 2.155, the anode still plays a hefty portion (24 wt.% and 16 vol.%, Figure 2d,e) in realizing a pouch-cell level energy density of 120 Wh kg⁻¹ and 555 Wh L⁻¹. At the same time, a limited N/P poses a challenge to the Zn reversibility and battery cycle life, as mentioned in Figure 1b. Therefore, pushing high reversibility of Zn stripping and plating is a must.

3.2. Zn Reversibility Needs to Balance Out AZMB Energy Density

Due to the current poor Zn reversibility, excessive Zn is a practical strategy to budget some battery life cycles from the energy density at the battery design level. However, the excess Zn does not release additional capacity but only a "reservoir" to compensate for the cycle-to-cycle Zn loss. An indulgent N/P can harm the energy density of the overall AZMBs.

Using flooded electrolytes is another overcompensating strategy to endure poor Zn reversibility. Although electrolyte is one of the battery essentials, it does not provide active capacity. Despite
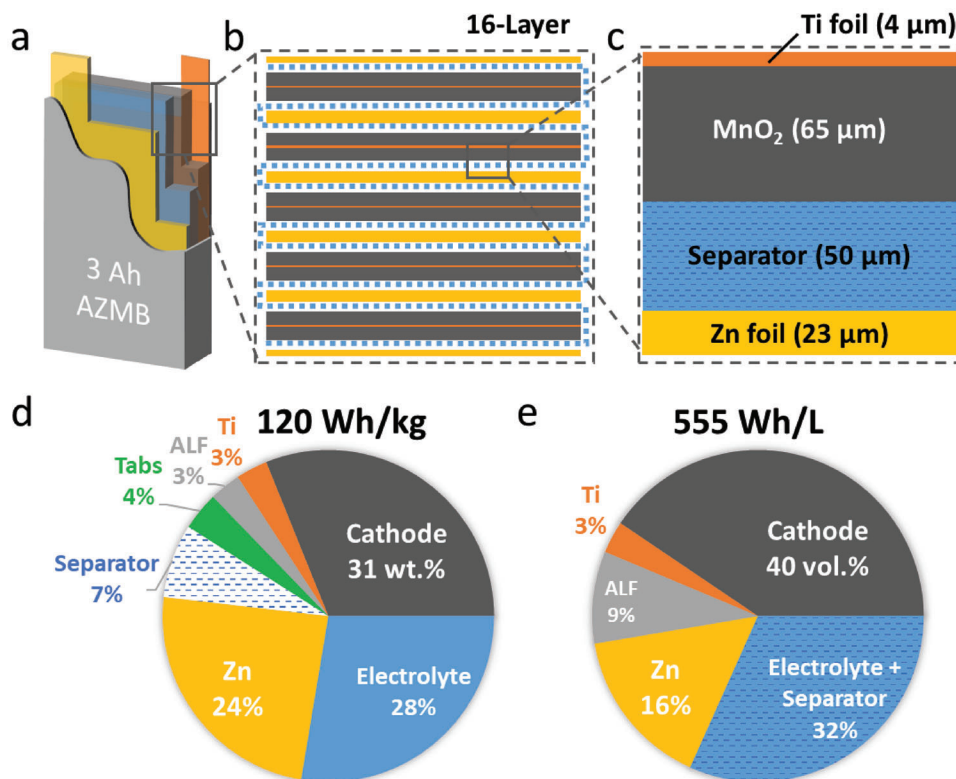
Figure 2. a) A pouch cell illustration. b) Stacking layers in an AZMB pouch cell and c) each layer's thickness. Cell-level d) mass and e) volume ratios of each main component in the projected AZMB.

the importance of electrolyte chemistry to the decline of side reactions at the interface, it is not well known that the amount of electrolyte also matters, as studies reported that a flooded electrolyte could trigger a fast cell impedance increase and a thick passivation layer.[35] Compared with reducing the N/P to <2, the lean electrolyte is considered a progressive approach to boost battery energy density. LMB pouch cell uses a lean electrolyte of E/C = 1.86 g Ah^{-1}.[36] For MnO$_2$/Zn, reducing E/C to <1.86 g Ah^{-1} can enhance the pouch-cell level energy density to 135 Wh kg^{-1} (**Figure 3**a). However, it is essential to note that the rapid depletion of lean electrolytes, compared with a flooded electrolyte

(such as 75 µL in a CR2032 coin cell), can introduce high polarization, high cell impedance, and low CE.

Moreover, to obtain a high volumetric energy density (E_V), for liquid electrolytes, a functional yet thin separator is essential. Reducing the thickness is the objective for beyond-liquid electrolytes, such as solid-polymer electrolytes (SPEs). As shown in Figure 3b, a 10 µm separator helps elevate the energy density of the MnO$_2$/Zn pouch to 745 Wh L^{-1}, and it is not unattainable given that a sub-5-µm SPE has emerged in the LMB field.[37] This E_V will make AZMB a competent candidate in the power-type battery market and large-scale energy storage applications.
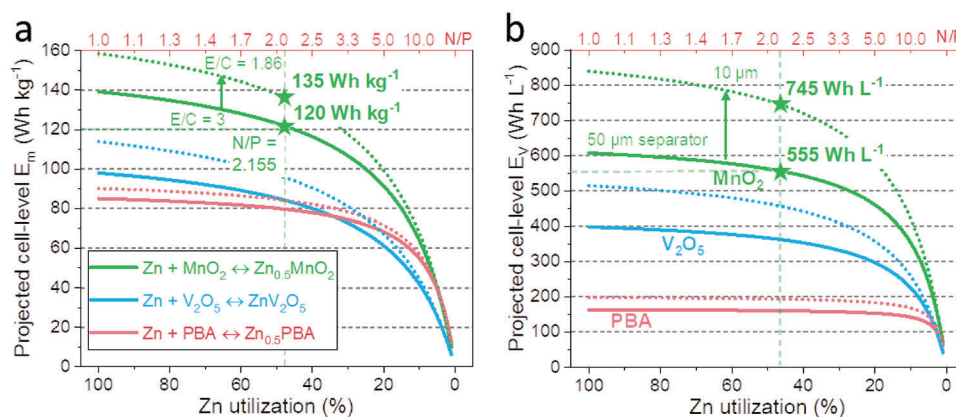

Figure 3. The pouch-cell level a) E_m and b) E_V were projected using three selected cathodes (MnO$_2$, V$_2$O$_5$, and Prussian blue analogs).

**ADVANCED
SCIENCE NEWS**

www.advancedsciencenews.com

**small
methods**

www.small-methods.com

Ambitiously, with an N/P = 1.1 that has only been achieved in LIBs[32] and a 5-µm-thick SPE, a MnO_2/Zn pouch cell has the potential to achieve an 865 Wh L^{-1} energy density.

3.3. Selection of AZMB Cathode

In addition to the Zn excess, electrolyte amount, and electrolyte thickness, the pouch-cell level energy density of an AZMB also varies by the selection of cathode material. Popular AZMB cathodes are MnO_2, V_2O_5, and Prussian blue analogs (PBAs). The characteristic specific capacity and operating voltage of each cathode material are summarized in Table S2 (Supporting Information).

As shown in Figure 3a, the MnO_2/Zn pouch cell is projected to achieve a 120 Wh kg^{-1} energy density with a feasible N/P = 2.155 and E/C = 3 g Ah^{-1}. A 135 Wh kg^{-1} MnO_2/Zn cell is attainable by reducing the E/C to 1.86 g Ah^{-1}. For V_2O_5 and PBA-based AZMBs, an 80 Wh kg^{-1} is attainable. However, no matter how high the Zn util.% is, neither can achieve an energy density above 100 Wh kg^{-1}.

For power-type batteries, a promising E_V is essential. MnO_2/Zn pouch cell generates a 555 Wh L^{-1} energy density and a possible 745 Wh L^{-1} if a sub-10-µm separator is developed for AZMBs (Figure 3b). It can be further boosted to above 800 Wh L^{-1} when N/P < 1.45. At the same time, V_2O_5 has the potential to show a >500 Wh L^{-1} energy density in AZMBs. However, the large-scale use or promotion of V_2O_5 cathodes needs to proceed with caution due to their toxicity to the human body[38] and the environment.[39] The vast space for PBA cathode can easily accommodate Zn^{2+} with fast kinetics, but the chance is minimal if the energy density of PBA/Zn AZMB needs to exceed 200 Wh L^{-1}.

3.4. Boosting the Energy Density of AZMB Pouch Cells

It is important to note that a high-energy-density AZMB pouch cell is only achievable in MnO_2/Zn chemistry using a controlled excess of Zn (small N/P), a lean electrolyte (small E/C), and a thin separator. A consensus on a development pathway for boosting the energy density of AZMBs needs to be built.

From a development perspective, a synergic improvement of different AZMB components is considered more economical than pursuing an N/P < 2 in the near future. For example, boosting the AZMB energy density from 120 to 130 Wh kg^{-1} (+7.7%) needs an N/P = 1.5 (−30% from 2.155). However, this minimal N/P ratio can bring a technological conundrum to battery stability. Using Li metal as the anode, the state-of-the-art LMB only has achieved an N/P of 2, despite years of studies and a stabler Li-organic interface with SEI formation than the $Zn-H_2O$ interface. Hence, compared with confining the room of Zn utilization, work on other battery components, such as a lean electrolyte, should be done beforehand to boost the overall E_m of AZMBs further.

Figure 4 shows a three-stage development trajectory for boosting the energy density of MnO_2/Zn AZMBs. The milestone of an N/P = 3.2 and an E/C = 9.3 has been achieved in a state-of-the-art AZMB pouch cell.[33] We propose a stage-I development plan for
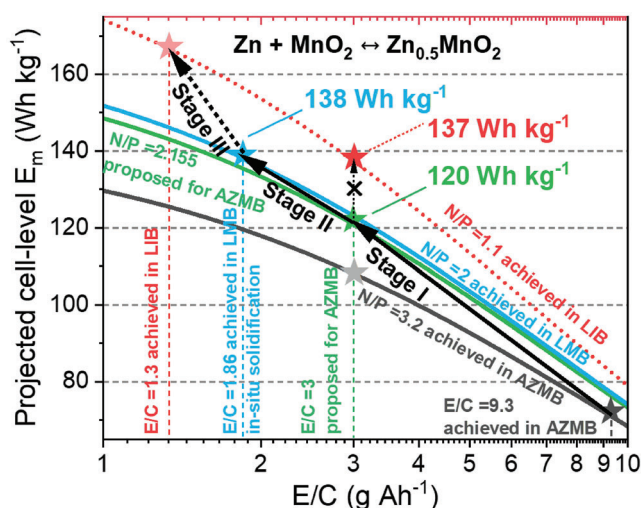

Figure 4. The development trajectory of MnO_2/Zn secondary battery.

a 120 Wh kg^{-1} AZMB (cathode loading = 6.78 mAh cm^{-2}, N/P = 2.155 and E/C = 3). With a 99.9% CE and a 2.155 N/P, a 1000-cycle battery can be projected. At this development stage of AZMBs, due to the instability of the $Zn-H_2O$ interface and the complexity of aqueous reactions, overcoming the technological barriers to achieve 99.9% Zn metal reversibility is ambitious enough. Stage II needs to accomplish the N/P = 2 and E/C = 1.86 that has been achieved in LMBs in AZMBs.[36] This will further boost AZMB energy density to 138 Wh kg^{-1}. Stage III needs to achieve the N/P = 1.1 and E/C = 1.3 that has only been achieved in LIBs using graphite anodes in AZMBs. From Stage II to III, compared with the economic investment in overcoming the present technological barriers in Zn metal anode, the benefits of cutting weight and volume from the N/P and E/C ratio can experience a "marginal effect" in the future.

4. An Overview of CE Determination Methods

4.1. Principles of CE Determination

CE is reported in either an asymmetric cell or a full cell in AZMB research. Symmetric cells give limited information about the battery's CE. It is well known that the CE tested in a full cell reflects the reversible capacity ratio out of the total discharge capacity, in other words, the reversibility of the battery chemistry. However, the implication of CE in an asymmetric cell context is not very well known.

An asymmetric cell uses Ti or Cu as the working electrode (WE) versus Zn. The CE of the Ti/Zn cell indicates the reversibility of Zn stripping and plating on the Ti substrate. In other words, it excludes either the beneficial or harmful effects of the cathode. Therefore, the asymmetric cell is widely used in Zn anode and electrolyte studies. Four CE (η) determination methods based on this configuration are widely used, as summarized in **Figure 5**. In an electrochemical context, they either use constant current (CC, galvanostatic) protocols[40] (Figure 5a–c) or a chronocoulometric CV method (Figure 5d). To be more exact, Figure 5a demonstrates a method in which a set capacity of Zn is galvanostatically plated
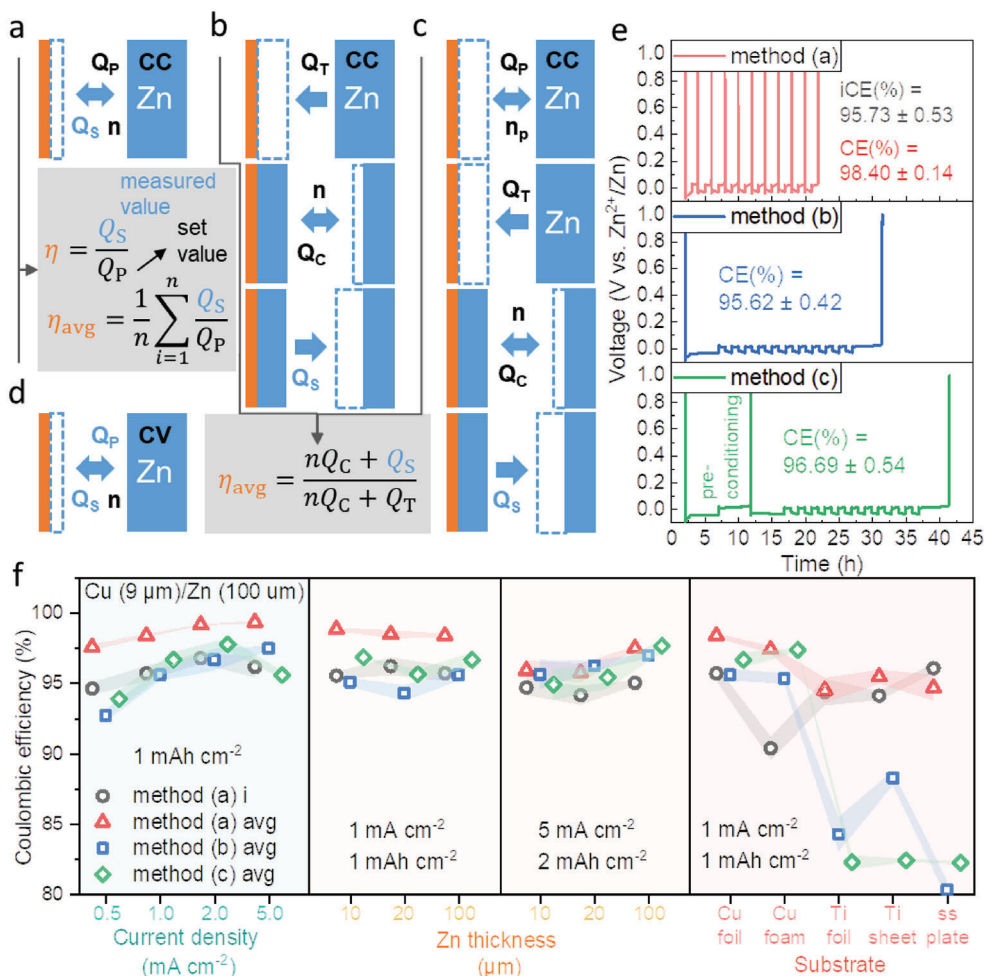
**ADVANCED
SCIENCE NEWS**

www.advancedsciencenews.com

**small
methods**

www.small-methods.com

Figure 5. a–d) A graphic summary of mainstream CE determination methods using asymmetric cell configuration. Reproduced with permission.[42] Copyright 2020, Zhengzhou University. For the values that appear in the equations, the set value, value to be measured, and value to be calculated are colored in black, blue, and orange, respectively. e) Experimental V–t profiles at 1 mA cm^{-2} and 1 mAh cm^{-2} of each CC method are demonstrated. f) Factors of current density, Zn thickness, and substrate type are investigated, and each is plotted with a shaded error bar.

onto a substrate, and the amount of Zn that can be stripped from the substrate is measured. This method gives both the CE of each cycle and an average CE via Equations 4 and 5. It is known that the initial CE is often quite limited compared with the following cycles. However, the CE result of this method is strongly related to the selection of substrate materials.

$$\eta = \frac{Q_S}{Q_P} \tag{4}$$

$$\eta_{avg} = \frac{1}{n} \sum_{i=1}^{n} \frac{Q_S}{Q_P} \tag{5}$$

Figure 5b shows a method in which a Zn-coated substrate is constructed first, and afterward, the Zn on the substrate is stripped and plated for cycles (n) before being entirely stripped at the last set cycle by charging to a set cut-off voltage. The point is to minimize the impact of the substrate by plating Zn onto the substrate. The CE calculation follows Equation 6. Figure 5c

adds a pre-conditioning step of plating at least 3 mAh cm^{-2} of Zn onto the substrate, followed by an entire stripping to remove oxidation layers on the substrate. This pre-conditioning step can diminish the lattice mismatch, alloying, and interphase effect on the substrate, stabilizing the later CE results.[41] The rest is identical to the method presented in Figure 5b. Therefore, these two methods share the same calculation (Equation 6).

$$\eta_{avg} = \frac{nQ_C + Q_S}{nQ_C + Q_T} \tag{6}$$

Figure 5d presents a CE test method that uses a voltage-controlled CV program. The plating and stripping capacities are measured, and the CE is calculated using Equation 5. Likewise, a pre-conditioning step of Zn coating or removal of the oxidation layer can be fitted to this CV program by adjusting the scanning speed. However, this method should be applied cautiously because the current density or areal capacity in a realistic battery cycling test cannot be fitted into the CV program.[41]

4.2. Reliability and Feasibility Analysis

Statistical analysis is applied to evaluate the reliability of each method and the degree of impact of each related factor in CE measurements (Figure 5e,f). It is found that CEs obtained using different substrates or testing methods are incomparable. Details are discussed further below.

1) *Test Method*: Statistically, the calculated CE value of each method comes with a deviation. The method that gives a CE value with a slight variation is considered accurate and repeatable. Figure 5e presents the tested values and their deviations using three galvanostatic methods (a), (b), and (c) at 1 mA cm^{-2} and 1 mAh cm^{-2}. Among all three methods, method (a) gives the highest average CE value with a minor deviation (98.40 ± 0.14%). The CEs tested using methods (b) and (c) are 95.62 ± 0.42 and 96.69 ± 0.42%, respectively.

2) *Areal Current and Capacity*: The relation of current density (0.5, 1, 2, 5 mA cm^{-2}) and tested CE with a set areal capacity of 1 mAh cm^{-2} are investigated, as shown in Figure 5f and Table S3. Different currents or areal capacities give varied CEs for the same thick Zn anode in all methods. For methods (a) and (b), a higher average CE is obtained under higher current densities. In contrast, method (c) and the initial CE tested by method (a) present a peak CE under 2 mA cm^{-2} cycling. The selected areal capacity can also impact the value and deviation of the tested CE. For a set current density of 5 mA cm^{-2}, a higher areal capacity of 2 mAh cm^{-2} gives a significantly higher CE of 97.67 ± 0.44% than 95.62 ± 0.28% at 1 mAh cm^{-2}. Method (a) gives a considerably smaller CE of 97.51 ± 0.15% than the 99.35 ± 0.09% at 1 mAh cm^{-2}. While method (b) shows little dependence on the areal capacity change (Table S4, Supporting Information).

For future studies, we suggest selecting similar areal current density and the areal capacity together with the Zn util.% for asymmetric CE test as in a full battery. Commercial AZMB pouch cell is expected to achieve a 6–7 mAh cm^{-2} capacity loading, which in return requires the Zn anode to endure a high areal current of at least 6 and 18 mA cm^{-2} at 1C and 3C, respectively. Especially for a test using high Zn util.% and high current density, methods (b) and (c) are preferred because the initial Zn loss in methods (a) can trigger an early voltage surge.

3) *Zn Thickness*: Zn thickness determines the extent of Zn excess. With a set areal capacity, the Zn util.% is determined (Equation 3). Figure 5f compares the measured CE using different thickness Zn versus Cu foil configurations. At a cycling condition of 1 mA cm^{-2} and 1 mAh cm^{-2}, the tested average CE values by method (a) are significantly higher than method (c), followed by method (b), regardless of Zn thickness (Table S5, Supporting Information). The pre-conditioning step positively affects constructing a stable interface on the Cu side. At 5 mA cm^{-2} and 2 mAh cm^{-2}, the tested CEs of all three methods become close (Table S6, Supporting Information). Especially method (b) presents stable CE output disregarding Zn thickness.

There was a misconception that there was no direct relation between the tested CE and Zn util.% if the same current is applied and the Zn reservoir is sufficient. Only the voltage surge arrives earlier than the set program due to Zn depletion (Figure S2, Supporting Information). However, this work presents that CE can vary with Zn thickness, as observed among all four methods (Figure 5f). Especially when the areal capacity of Zn stripping and plating is set high, the effect of Zn thickness becomes non-neglectable. In addition, the nuance of the crystal structure of different-thickness Zn can arguably be due to their different calendaring processes from a manufacturing perspective. For example, Chen et al. reported an annealed and cold-calendared Zn presenting a higher (002) percentage on the surface than the pristine and improved striping and plating reversibility.[43] However, to which degree the calendaring can impact the Zn structure and what calendaring procedure can maximize the Zn reversibility are yet unknown.

Despite the possibly poor CE with a thin Zn foil, it is suggested to use a controlled N/P ratio. For example, a 20 µm Zn provides an 11.7 mAh cm^{-2} areal capacity that is expected to match a 4 mAh cm^{-2} cathode (N/P = 2.9) in a full AZMB. Considering most research uses a small to medium cathode loading of <3 mAh cm^{-2}, <20 µm Zn is suggested for all CE tests in both coin and pouch cell configurations.

4) *Substrate*: Debates about substrate materials still exist. Table S7, Supporting Information shows that Cu foil is a low-cost, soft, and ultra-thin substrate, while Ti and ss have high cut-off voltages of >2 V versus Zn^{2+}/Zn. Especially, Ti is favorable in boosting the energy density of a battery due to its light density and can meet the requirements to reflect the issues associated with high voltages and the high water activity in the electrolyte. Yu et al. investigated various current collector materials' ESWs in an aqueous electrolyte and found that Ti mesh maintains a wide ESW, contributing to a minimal irreversible capacity of <2% from chemical reactions among the basic, neutral, and acidic electrolytes.[44]

However, Ti (Figure S3d,e, Supporting Information), as well as ss, Al, and Ta (Figure S4a–c, Supporting Information), gives a "wobbling" voltage-time profile, ascribing to an orphaning effect.[45] As shown in Figure S5b,c (Supporting Information) ss and Ti both show sudden potential drops and unstable charge voltages reflecting a strong orphaning effect, where metal deposits are constantly disconnected from the electron source at the electrode, and the "dead" fragments are randomly reconnected.[45] Orphaning metal deposits present as loose particles stuck in the separator and can be observed by microscopy (Figure S2, Supporting Information). Although it is exciting to have a substrate material that can endure a cut-off voltage as high as possible, specifically for CE tests that are expected to present the reversibility of Zn stripping and plating, studies have suggested that a 0.5 V (versus Zn^{2+}/Zn) endurance is sufficient for a substrate,[41] as Zn stripping from the substrate should have been completed by 0.2 V, especially in diluted aqueous electrolytes.

The Zn^{2+}/Zn redox potential in regular aqueous liquid-state electrolytes should only fluctuate by no more than ±100 mV due to concentration polarization at even a relatively high current density. However, if the Zn stripping plateau is not completed by 0.5 V or a new side-reaction plateau appears by 0.5 V, the substrate material needs to be changed due to overlapped signals from either dissolution, alloying, or orphancy effect.

**ADVANCED
SCIENCE NEWS**

www.advancedsciencenews.com

**small
methods**

www.small-methods.com

Zheng et al. observed inactive deposits in Au/Zn, which are found to be the intermetallic phase AuZn.[46] They believe that noble metals such as Au and Ag present a thermodynamically favorable alloying behavior, a diffusion-controlled bulk conversion, while (de-)alloying with Zn.[46] Because of that, their body structures become porous during the secondary plateau (0.3 and 0.2 V, respectively) of de-alloying in charge (Figure S4e,f, Supporting Information). In contrast, Cu undergoes a moderate "pseudo-capacitive" alloying that occurs only at the interface and does not affect their body structures.

It is worth noting that for gel polymer or solid polymer electrolyte, due to the high internal resistance, the battery polarization can lead to a >0.5 V overpotential at high currents. In this work, Cu foil (9 μm, single-abrasive) provides the highest CE of Zn stripping and plating with a slight deviation (98.40 ± 0.14%, Figure 5f, Table S8, Supporting Information) and presents impeccable stability under a cut-off voltage of 1.0 V (Figure S3a, Supporting Information) among all substrates. Lynden et al. reported the CE distinction of Zn electrodeposition on different substrates and ascribed it to the hardness of substrate materials impacts the Zn stripping and plating reversibility.[46] Cu (51, Rockwell B-scale) is softer than Ti (80) and ss 304 (88). A soft substrate can neutralize residual forces and contribute to Zn homogeneity.

Metal foil and foam do not share the same body structure and surface energy. Experimentally, the initial CE using Cu foam (90.42 ± 0.82) is significantly smaller than Cu foil (95.73 ± 0.53, Table S7, Supporting Information). However, as the cycle number increases, CEs in both cells are improved. As mentioned before, the physiochemical properties of substrate materials should mimic the cathode material. Therefore, an abrasive Cu foil is favorable, considering the cathode in a full battery after hot rolling has a dense body yet an abrasive surface. Cu foam is too porous in this case.

In summary, Cu foil is the most favorable substrate to measure the CE of Zn electrodeposition. Especially considering that Cu foils have been widely used in LMBs, they are commercially available and technologically mature. The abrasive side should face Zn. An average CE with a deviation <0.1% from at least four parallel trials should be reported. The impact factors of future substrate selection are categorized below. However, the substrate species' natural source of the CE deviation created needs further study.

a) Mechanical properties of the substrate, such as thickness,[46] hardness, and surface roughness;
b) Electrochemical stability (redox resistance), electron conductivity, purity;
c) Surface topography (bare versus coated), body structure/morphology (foam versus foil).

Moreover, as mentioned before, the substrate should match the selected cathode materials. Nevertheless, the word "match" and matching in which property is unclear. Idealistically, the substrate should share identical mechanical and physiochemical properties with a selected cathode, and the cycling program should use the same charge and discharge window. However, this is barely possible and deviates from the initiative of the CE test in asymmetric cell configuration. We believe that feasibility and repeatability should still be put in the first place: CE should still act as a fast method to understand the Zn stripping and plating reversibility, and the result should be repeatable with a slight deviation.

Previously, it was widely believed that the initial CE is smaller than sequential cycles. However, this work found an abnormal CE decrease by cycle in Ti/Zn or ss/Zn cells (Figure S3c–e, Supporting Information). A possible reason is that their intrinsically hard body and non-abrasive surface accelerate the Zn detachment from the substrate, which becomes "dead Zn," with an irreversible capacity shown in the electrochemical profiles. During the charging process, ss voltage (Figure S5b, Supporting Information) shows a strong oscillation at ≈1.0 V, indicating an alternation of active Zn plating (voltage surge) and dead Zn detachment (voltage drop).

Furthermore, in an anode-free battery, the CE tests in an asymmetric cell configuration identically reflect the Zn plating and stripping reversibility on a heterosubstrate.[46] Similarly, for future AZMB anode, instead of using fragile Zn foil, Cu foil is a state-of-the-art metallic substrate for preparing Zn-electrodeposited anode.

5) *Temperature*: It is crucial to have a consistent temperature during CE testing because unmodified aqueous electrolytes often present relatively narrow working voltage windows. A temperature of 0 °C can turn a dilute aqueous electrolyte into a solid state, whose ion mobility is entirely different, and the CE of any high- or low-temperature compatible AZMBs should be discussed separately.

5. State-of-Art CEs in AZMB Research

5.1. CEs Reported in Asymmetric Cells

Table 2 summarizes the state-of-the-art CE reported in an asymmetric cell configuration. Especially electrolyte modifications and electrode coatings are effective CE improvement strategies. For example, $Me_3EtNOTf$[4b] and $La(NO_3)_3$[8] are successful additives for $Zn(OTf)_2$ and $ZnSO_4$ aqueous electrolyte, respectively, presenting an average CE of ≥ 99.9%. A eutectic electrolyte of $Zn(TFSI)_2$/acetamide (1:7 mol.) also presents a 99.9% CE in Ti/Zn cells using method (d).[47] The covalent organic frameworks (COFs) are promising protective coating materials that have achieved an ultra-high CE of 99.95%.[48] Studies commonly use a small Zn utilization of <1%, and method (a) remains the most popular to determine the CEs. In fact, realistic test conditions require a Zn util.% of 33% (N/P = 3 at maximum) for future CE studies.

5.2. CEs Reported in Full Cells

The initial CEs of AZMB full cells are summarized in **Table 3**. The irreversible capacity loss in a full cell configuration is attributed to some unfavorable parasitic reactions at the interface, such as corrosion, passivation, and cathode dissolution, that "poisons" active Zn and produces gas, liquid, and solid by-products. Electrochemically, this reflects an inhomogeneous electrodeposition where Zn "dendrites" are stimulated and deactivated into "dead" Zn, leading to a permanent capacity loss.

As shown in Table 3, the highest CE (99.8%) has been achieved in K_zMnO_2//1 M $Zn(OTf)_2$ + 1 mM SDS in H_2O//Zn_xCu_y@Zn

Table 2. State-of-the-art CE reported in asymmetric cells.

Electrolyte[a]	WE/CE	CE [%][b]	I [mA cm^{-2}]	Q [mAh cm^{-2}][c]	Zn util.%	Voltage [V]	Method	Reference
1 м Zn(OTf)$_2$	AgNPs@CC/Zn	91.3	5	2	–	0.5	a	[52]
		98.1 (10)						
		99.1 (30)						
		99.5 (50)						
		99.5 (800)						
		99.5	10	1		0.5	a	
1 м Zn(OTf)$_2$ in H$_2$O/ACN (3:1 vol.)	Cu/Zn	99.3	1	1	–	0.5	a	[53]
1 м Zn(OTf)$_2$ in AN/H$_2$O (72:28 vol.)	Cu/Zn	96.14 (25 °C) 99.53 (−40 °C)	0.5	5+1×9	–	0.5	b	[54]
2 м Zn(OTf)$_2$	Cu/SEI@Zn	99.5 AVE	1	1	–	0.5	a	[55]
3 м Zn(OTf)$_2$	Ti/ZnAl@Cu-mesh	99 (50)	1	1	–	0.5	a	[56]
3 м Zn(OTf)$_2$	Ti/60alucone@Zn	98.6 (10)	0.5	0.5	–	1.0	a	[57]
3 м Zn(OTf)$_2$ + (H$_2$O-HAc)/TMS	Cu/Zn	99.25	1	5×1+5+1×30	5.70	0.6	c	[58]
4 m Zn(OTf)$_2$ + 0.5 m Me$_3$EtNOTf	Ti/Zn	**99.9 (100)**	0.5	0.5	–	0.5	a	[4b]
1 м Zn(TFSI)$_2$-TFEP @MOF	Ti/Zn	99 (80)	0.5	0.5	–	0.5	a	[59]
		99.5 (130)						
		99.9 (300)						
		99.1 (350)						
1 м Zn(TFSI)$_2$-AN	Ti/Zn	87.3	0.2	0.1	–	0.5	a	[60]
		99.5 (10)						
Zn(TFSI)$_2$-acetamide (1:7 mol.)	Ti/Zn	91.9	1 mV s^{-1}	≈0.61	–	−0.5–1.2 V	d	[47]
		98.6 (15)						
		99.5 (30)						
		99.9 (50)						
4 м Zn(TFSI)$_2$	Cu/Zn	97.5	1	4+0.4×20	–	0.5	b	[61]
LZ-DES•0.3H$_2$O LZ-DES = LiTFSI/Zn(TFSI)$_2$/urea (1:1/20:1/1.32 mol.)	ss/Zn	96.2 (11)	0.5	0.5	–	0.5	a	[2]
0.1 м Zn(TFSI)$_2$ in FM/DFM (1:1 mol.) + 1 mol.% MP	Cu/Zn	99.3	0.5	5+1×9	20	0.5	b	[62]
2 м Zn(BF$_4$)$_2$ – [EMIM]BF$_4$	ss/Zn	99.36 AVE	0.5	0.5	–	0.5	a	[63]
0.5 м ZnSO$_4$	Ti@rece-SO$_4^{2-}$/Zn	97.61 AVE	0.5	0.25	0.43	1.0	a	[64]
1 м ZnSO$_4$	PVB@Cu/Zn	83.5	1	0.5	–	0.5	a	[65]
		99.4 AVE	4	2				
1 м ZnSO$_4$ in H$_2$O/ACN (3:1 vol.)	Cu/Zn	99.6	1	1	–	0.5	a	[53]
1 м ZnSO$_4$ in H$_2$O/EG/MeOH (70:6:24 vol.)	Ti/Zn	99.3	2	2	3.42	1.0	a	[66]
2 м ZnSO$_4$	β-PVDF@Cu/Zn	96.9 (30)	0.36	0.18	–	0.5	a	[67]
		96.5 (200)						
2 м ZnSO$_4$	ZnF$_2$-Cu/Zn	90.89	0.5	20+0.5×100	1.71	–	b	[68]
2 м ZnSO$_4$	Cu/NTP-C@Zn	92.75	0.38	0.19×1+1.52+0.38×15	0.68	0.5	c	[69]
2 м ZnSO$_4$ in EG/H$_2$O (2:3 vol.)	Ti/Zn	98 (25 °C) 99 (−20 °C)	2	1	–	0.5	a	[70]
2 м ZnSO$_4$ + 0.08 м ZnF$_2$	ss/Zn	99.71	40	1.2	–	0.5	a	[71]
		99.64		1.8				
		99.60		2.4				
		99.58	10	0.6				
		99.53	20					
		99.87	30					
		99.68	40					

(Continued)

ADVANCED
SCIENCE NEWS

www.advancedsciencenews.com

small
methods

www.small-methods.com

Table 2. (Continued)

Electrolyte[a]	WE/CE	CE [%][b]	I [mA cm^{-2}]	Q [mAh cm^{-2}][c]	Zn util.%	Voltage [V]	Method	Reference
2 м ZnSO$_4$	Cu/Zn	97.32	1	1	1.71	–	a	[72]
+ 0.025 м 2-Methylimidazole		98.93	8	8	**13.7**			
2 m ZnSO$_4$	Cu/Zn(002)	97.71	1.13	0.565+0.2825×10	0.10	1.0	b	[73]
	Cu/Zn(100)	95.12						
2 m ZnSO$_4$	DIPD@SS/Zn	99.95 AVE (>12)	4	1	0.68	0.8	a	[48]
2 m ZnSO$_4$ + 0.0085 m La(NO$_3$)$_3$	Ti/Zn	99.9 AVE	2	1	2.14	0.4	a	[8]
3 м ZnSO$_4$	Ti@SR/Zn	99.07	0.5	5+0.5×30	0.85	1.0	b	[64]
0.2 м ZnCl$_2$	Au/Zn	99.9 AVE	0.05 V s^{-1}	–	–	–0.5–0.8 V	d	[74]
0.5 м ZnCl$_2$	Cu/Zn	93.89	5	5×1+5+0.5×10	1.07	0.5	c	[75]
0.5 м ZnCl$_2$ + 2.5 м Choline-Cl	Cu/Zn	96.19	5	5×1+5+0.5×10	1.07	0.5	c	[75]
1 м ZnCl$_2$	Ti/Zn	92.0 AVE	1	0.5	0.34	0.5	a	[76]
5 m ZnCl$_2$	Ti/Zn	73.2	1	4×1+4+0.4×100	0.68	–	c	[77]
30 m ZnCl$_2$		95.4						
30 m ZnCl$_2$	Ti/Zn	98.4	1	4+0.4×100	–	–	b	[78]
7 м ZnCl$_2$	Ti@SR/Zn	95.42	0.5	5+0.5×30	0.85	1.0	b	[64]
7.5 м ZnCl$_2$	Cu/Zn	97.93 (25 °C)	0.2	1+0.2×9	–	0.5	b	[79]
		99.52 (−70 °C)						
7.6 m ZnCl$_2$	Ti/Zn	97.0 AVE	1	0.5	0.34	0.5	a	[76]
7.6 m ZnCl$_2$ + 0.05 m SnCl$_2$	Ti/Zn	99.7 AVE	1	0.5	0.34	0.5	a	[76]
30 m ZnCl$_2$ + 5 m LiCl	Ti/Zn	99.7	1	4+0.4×100	–	–	b	[80]
ZnCl$_2$:TEHC:H$_2$O (1:3:80 mol.)	Ti/Zn	90	0.5	1	–	0.5	a	[81]
		98.9 (9)						
1 м Zn(ClO$_4$)$_2$	Cu/Zn	99.3	2	4×2+4+0.5×50		0.5	c	[82]
PMC hydrogel	Cu/Zn	83.7	1	2	3.42	0.5	a	[83]
		99.5 AVE						
PAMPS-Zn hydrogel	Cu/Zn	87.5	1	1	1.71	0.5	a	[84]
		99.3 AVE						

[a] Only salt and their concentration are noted when water is the only solvent. Dependent on the electrolyte preparation method, either molarity (mol L^{-1}, м) or molality (mol kg^{-1}, m) is used to note the concentration of salts; [b] Method (a) report 1st CE, or CE (cycle number), or CE (AVE). Methods (b) and (c) only report average CE; [c] Method (b) uses Q_T (mA cm^{-2}, if different) + $Q_C \times n$. Method c uses $Q_P \times n_P + Q_T + Q_C \times n$.

system at 0.2C.[49] Acetonitrile has been presented as an effective and low-cost co-solvent in Zn(OTf)$_2$-H$_2$O electrolyte, leading to a presentable CE of 99.7% at 0.1C in a MnO$_2$//Zn full cell.[50] NASICON-type polyanion cathodes also present a promising CE of 99.7% in a Na$_3$V$_2$(PO$_4$)$_2$O$_{1.6}$F$_{1.4}$//25 m ZnCl$_2$ + 5 m NH$_4$Cl//Zn battery at 0.5C.[51] As discussed previously, a 120 Wh kg^{-1} MnO$_2$/Zn pouch cell requires at least 99.9% CE to guarantee a 1000-cycle life. In order to achieve this, synergetic improvements of the cathode, Zn metal, and electrolyte are needed.

In this CE test framework, we suggest first testing in a Cu/Zn asymmetric cell using method (a) to fast and accurately measure the Zn stripping and plating reversibility and see the CE variation by cycle, then testing in a coin-cell type (stacked by PP if multi-layer) full battery, lastly in a pouch-cell type (single layer to multi-layer) full battery. In full batteries, the depth of discharge controlled by cut-off voltage and current needs to be optimized to obtain good CE and cycling stability.

6. CE Improvement Strategies

The CE improvement of AZMBs needs efforts from all components. The underlying mechanisms need to be studied. Mean-

while, the scalability and cost-effectiveness of a strategy should be evaluated. Below are summarized the CE improvement strategies reported in AZMBs and similar battery chemistries that are transferrable to boost the reversibility of future AZMBs.

1) *Zn Engineering*
   a) Surface Energy Mitigation: thermal heat (high-temperature annealing to remove residual forces and construct (002)-dominant crystalline orientation),[43] pressure (change body structure), UV light (change TiO$_2$ coating's hydrophilicity),[96] soft substrate (carbon cloth, carbon sheet, graphite sheet),[97] surface polishing,[98] plasma cleaning;[99]
   b) 3D Micro/Nano-structuralizing: mechanical texturing,[28] Zn powder,[86,100] Zn alloy,[101] dilute acid corrosion,[102] laser texturing;[103]
   c) Defect Site Construction: hetero-cation doping,[97] plasma sputtering,[104] epitaxy regulation.[105]
2) *Heterointerface Construction*: The interface's chemical environment is related to electrolyte permeability and Zn deposit detachment. The thin-film techniques are:

ADVANCED
SCIENCE NEWS
www.advancedsciencenews.com

small
methods
www.small-methods.com

Table 3. State-of-the-art initial CE reported in full cells.

Electrolyte	WE/CE	CE [%]	Current [A g^{-1}]/C-rate	Capacity [mAh g^{-1}] D/C	Voltage window [V]	Zn util.%	Reference
1 м $ZnSO_4$ + 0.1 м H_2SO_4	MnO_2/Zn	98.5 (10)[a]	30 mA cm^{-2}	1.3/2 mAh cm^{-2}	0.8/2.2[b]	–	[85]
2 м $ZnSO_4$ + 0.1 м $MnSO_4$	MnO_2/Zn(P)[c]	77 / 99 (10)	3	129/168	1.0/1.9	–	[86]
2 м $ZnSO_4$ + 0.1 м $MnSO_4$	MnO_2/ SPEEK@Zn	99 AVE	0.1	271/294	0.8/1.8	–	[87]
2 м $ZnSO_4$ + 0.08 м ZnF_2	LMO/ss	81.25 / 98.75 AVE	0.2	78/96	1.4/2.1	–	[71]
1 м $Zn(OTf)_2$ + 1 mM SDS	K_zMnO_2/Zn_xCu_y@Zn	99.2 / 99.8	5 / 0.2	164/165 / 319/320	1.0/1.8 / 1.0/1.8	0.22 / 0.43	[49]
$Zn(OTf)_2$ in H_2O/AN	MnO_2/Zn	99.7 AVE	0.03 /0.1 C	200/280	0.8/2.0	–	[50]
3 м $Zn(OTf)_2$ + 0.1 м $Mn(OTf)_2$	MnO_2/TiO_2@Zn	98.0 (20)	0.1 /0.65 C	235/240 (20)	0.8/1.8	–	[88]
1 м $ZnSO_4$	$Zn_{0.25}V_2O_5·nH_2O$/Zn	99	4.5 /15 C	≈200/-	0.5/1.4	–	[89]
3 м $ZnSO_4$	V_2O_5/Zn	94 99 (2)	0.1	352/374	0.3/1.6	–	[90]
1 м $Zn(OTf)_2$ in H_2O/PEG (3:7 wt.)	V_2O_5/Zn	≈100 AVE (200-250)	15	≈200/-	0.2/1.6	–	[91]
0.5 m $Zn(ClO_4)_2$ +18 m $NaClO_4$	$NaV_3O_8•nH_2O$/Zn	>99	4	>80/-	0.3/1.5	–	[92]
3 м $Zn(OTf)_2$	PEDOT-NVO/Zn	96.5	0.2	282.5/290.6	0.4/1.6	–	[93]
3 м $Zn(OTf)_2$	VOH/Zn	99.5	0.5	354.8/353.2	0.2/1.6	–	[94]
2 м $Zn(OTf)_2$ in H_2O/PC (2:1 mol.)	$Zn_xH_yVPO_4F$/Zn	≈100 AVE	0.028 /0.2 C	≈140/-	0.2/2.1	2.4	[95]
25 $ZnCl_2$ + 5 m NH_4Cl	$Na_3V_2(PO_4)_2O_{1.6}F_{1.4}$/Zn	99.7	0.5	155/-	0.4/2.1	–	[51]

[a] This is after 10 cycles of charge and discharge activation at 4 mA cm^{-2}; [b] This battery is charged by chronoamperometry at 2.2 V versus Zn^{2+}/Zn and galvanostatically discharged; [c] Zn powder made free-standing anode.

a) Dip/Spin Coating: coating materials can be polymers,[67,106] metal-organic frameworks (MOFs), and covalent-organic frameworks (COFs);[48]

b) Chemical Vapor Deposition (CVD): atomic layer deposition (ALD), molecular layer deposition (MLD);[57,107]

c) Physical Vapor Deposition (PVD): magnetron sputtering;[108]

d) In Situ Chemical Reactions: artificial SEI construction.[109]

3) *Electrolyte Modification*: Developing high-performance and cost-effective electrolytes and exploring the fundamental mechanisms of electrolyte chemistry are essential. The composition of electrolyte chemistry is widely known as salt, solvent, and additives. The salt can be subcategorized into cations and anions. Cations must include Zn^{2+} as they are the charge carriers in AZMB electrolytes. Anions and solvents are essential to forming a functional "solvation sheath" for ion transport and possibly an SEI for the anode.[1] Despite the narrow ESW of water making it difficult to decompose salt anions and generate an SEI, studies reported additives that make SEI formation possible in AZMBs.[31]

Based on each component of the electrolyte, strategies are summarized below:

a) Heterocations[8]: guide Zn electrodeposition via electrostatic shield effect at the anode "tips" or "escort" effect at interfacial electrolyte. Simultaneously, the shielding effect can also be active in ameliorating cathode dissolution;

b) Fluorinated Anions: help generate high-ZnF_2 artificial SEI at the first-cycle oxidation;[4b,55]

c) Multi-Solvent: constructs stable solvation sheath and prevents water reduction;[50]

d) Additives: some organics and gases can help regulate the crystallographic orientation of Zn deposition;[110]

e) Beyond-Liquid Electrolytes: they, such as hydrogels, gel polymers, and all-solid-state inorganic electrolytes, transport Zn^{2+} and regulate Zn growth by different mechanisms.[83–84]

The development of AZMB electrolytes witnessed a transition from dilute electrolytes to ultra-high-concentration electrolytes. Deep eutectic solvents and ionic liquids are hot topics in AZMBs. Locally-high concentration electrolytes are to be developed. While on the opposite, due to the cost benefits and low viscosity (thermodynamics), the ultra-diluted electrolyte has vast potential and should be investigated more.

Eventually, scientists and engineers need to reach a balance between high performance and cost-effectiveness. Due to the different effects of a battery, scientists study electrolytes as interfacial and body electrolytes. The interfacial electrolyte is involved in the electrochemical reaction, while the body electrolyte determines the ionic transport between the cathode and the anode. It is essential to project a particular application scenario while developing new electrolytes.

4) *Separators*: Envisioning the impact of separators on the CE of a battery is not always intuitive. Separators undertake three main functions:

a) Media of liquid electrolyte that facilitates ion transfer in body electrolyte;

b) Interface with an electrode that insulates electron transfer between cathode and anode;

c) Their body structures guide ion diffusion and resist dendrite penetration.

2300660 (11 of 16)

**ADVANCED
SCIENCE NEWS**

www.advancedsciencenews.com

**small
methods**

www.small-methods.com

Both energy- and power-type batteries require a functional separator to be as light and thin as possible. At the same time, the realization of the three functions needs a robust separator with strong mechanical strength and proper body structure.

5) *Cathode Modification*: In a full battery, cathodic dissolution can drastically reduce a battery's reversible capacity. Besides using electrolyte additives such as transitional metal salt, fine-tuning the structure of active materials is the key to success. An elastic and stable structure elevates the reversibility of electrochemical reactions. Heteroatom modification is widely used for LMB cathodes and is a feasible method to stabilize the active material structure and improve its electrochemical performance. All these structural modifications are expected to accommodate Zn^{2+} more reversibly.

Among all the strategies mentioned above, the authors consider a high-performance interface/interphase to be the key to elevating Zn metal reversibility. However, the electrolyte that boosts Zn reversibility the most could become a disappointment when we test it in full cells. Due to the complexity of cathode and anode interfacial instability, expecting a "panacea" electrolyte to resolve both-side issues is unrealistic, and studying cathodic and anodic interphase chemistries separately is strongly suggested. For Zn anode, modification of the body structure of Zn metal, such as using Zn powder base anode, has been proven superior CE in many studies. For the cathode, developing new materials with high electron conductivity and inelastic structure is essential. Ex situ coating methods like dip/spin coating and ALD/MLD featuring functional interphase for cathode and anode surfaces for different purposes and minimizing side reactions become favorable. In situ solidification of traditional liquid electrolytes is another promising method of improving interface stability.

7. Perspectives on Future AZMB studies

We suggest future studies pushing the battery chemistry further on a practical configuration basis. The development points are summarized in **Figure 6**.

1) *Realistic Test Conditions and Energy Density Improvements*
   a) Cathode Loading and Porosity: a >3 mAh cm^{-2} cathode capacity is suggested for all lab-scale AZMB research. Given that high loading gives a smaller specific capacity than small loading, taking a >3 mAh cm^{-2} V$_2$O$_5$ cathode as an example, a mass loading of >15 mg cm^{-2} should be expected. Additionally, hot rolling should always be applied to obtain a proper porosity that can show dual benefits – to facilitate the electrolyte permeability and minimize the detachment of active materials. More importantly, the loading and porosity need to be balanced. High loading aims for high areal capacity. A designed porosity should compensate for the inferior kinetics due to the low critical conductivity of the cathode material.
   b) Slurry Composition: Current lab-scale AZMB cathodes only contain 70–80% active materials. However, to avoid the unnecessary thickness of a high-loading cathode, minimizing the percentage of active carbon and increasing the percentage of active materials are essential. Industrial energy-type LMB cathodes contain 96–96.5%[32,36,111]
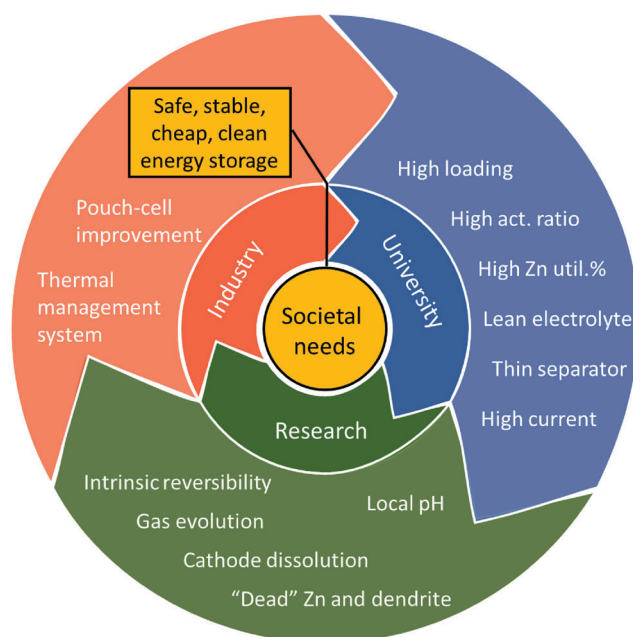

Figure 6. The developing points in AZMBs in a framework of Industry-University-Research associated with societal needs.

of active materials. For lab-scale studies, we suggest using >85% of active materials.
   c) Zn Thickness: To match with a 3 mAh cm^{-2} mild-loading cathode, a 15 μm Zn (N/P = 3) is suggested (Table S8, Supporting Information). A low N/P ratio is preferred to boost the energy density. Given the mundane reversibility of Zn due to the unsolved parasitic reactions in AZMBs and the high water activity of aqueous electrolytes, an N/P = 2.5–3 is suggested for all AZMB studies. When the reversibility is improved, the thickness of Zn can be further reduced.
   d) Lean Electrolyte: Instead of a flooded electrolyte in a coin cell (75 μL), an E/C ratio <3 g Ah^{-1} lean electrolyte is suggested in AZMB pouch cells due to a balanced cost-benefit and high performance.[32] Additionally, Due to the small amount of electrolyte, a general high-performance electrolyte should be able to maximize its permeability in a dense cathode. Other properties, such as ESW and TSW, should be improved explicitly for aqueous electrolytes with specific purposes. The core strategy of ESW improvement for aqueous electrolytes is decreasing the water reactivity and avoiding direct contact between electrode and electrolyte via hydrogen bond constraining water mobility and hydrophobic interphase formed on electrolyte, respectively.[20b] In addition, a proper pH can facilitate reaction kinetics and improve the reversibility of battery chemistry;[112] a high ionic conductivity is prevalently required. From a performance perspective, non-aqueous systems should be investigated. However, balancing out high performance against low-cost and green chemistry is a time-honored challenge.[113]
   e) Separator: A thin and light but reliable separator is needed for AZMBs. Commercial 20–25 μm Celgard polypropylene (PP) separators work well for LMBs; however, they do not

**ADVANCED
SCIENCE NEWS**
www.advancedsciencenews.com

**small
methods**
www.small-methods.com

work for AZMBs. Glass fibers are reliable separators for AZMBs, but their thickness of 260–675 μm brings an issue to the overall energy density of the battery. Studies have successfully demonstrated some thinner separators, such as polyacrylonitrile (69 μm),[114] commercial Nafion 212 (50.8 μm),[115] working in AZMBs. Additionally, it is worth noting that the difficulty of reducing the E/C ratio in AZMBs lies in the limitation of separator choices. A recent study reported a 9 μm ultra-thin PP@MOF separator for a 350 Wh kg^{-1} lithium nickel-cobalt-aluminum oxide (NCA)/Li battery with a minimal E/C = 1 g Ah^{-1}.[116] Studies have also developed an ultra-thin SPE with a thickness of 5 μm for LMBs.[117]

f) Realistic Currents: Pouch cell requirements guide symmetric cell testing protocols. The C-rate for stationary energy storage of LIBs is usually 0.5–2C[118] and not >10C.[119] Depending on the cathode loading, the Zn symmetric cell testing should use a current density of no more than 10 mA cm^{-2} to match a 5 mAh cm^{-2} cathodes. Thus, developing a promising Zn anode that can endure a 10 mA cm^{-2} current with decent stripping and plating reversibility is significant. In addition, the current density is a kinetic factor of the electro-decomposition of water. High current accelerates the H_2 evolution. Moreover, the high polarization in high-rate tests can harm the completion of a redox reaction with a decreased capacity in the regular voltage window.

2) *Pouch-cell Level Improvement*

More research on AZMB pouch cells and experimental data support are needed. Different battery configurations are utilized for different purposes and have varied structures (Figure S6, Supporting Information).[120]

Multi-Layer Pouch Cell:

a) Stacking Layers: winding is more used in cylindrical cells (Figure S6b, Supporting Information) and prismatic (Figure S6c, Supporting Information) or with a hard battery case. This method unavoidably induces edges that do not contribute enough capacity. Stacking is used in pouch cell configurations (Figure S6d, Supporting Information).

b) Rated capacity: the minimum experimental capacity the battery can release at suggested discharging conditions should be noted.

c) Interdisciplinary Studies: thermal management system (TMS), tab heat (all-tab cylindrical cells by Tesla versus single-tab), thermal runaway (prevention and monitoring).

3) *Mechanistic Studies on Zn Behaviors*

a) There is a need for more fundamental research and advanced techniques (mass spec titration to quantify inactive Li[121]). From EC profile (electrochemistry) to predict Zn behaviors (if correlated). Develop and tailor electrochemical methods for AZMB studies. Local pH variation and their correlation with gas generation (Figure S7, Supporting Information)[44] and Zn deposition behaviors should be further studied. Cao et al. reported that the $Zn(OTf)_2$ concentration impacts the pH of body electrolytes.[4b]

b) Gas Evolution: needs more attention and research. Challenges: gas evolution, electrolyte, Zn, modification method – their association is still unclear and should be studied. We need more focus on this because gas in electrolyte significantly impacts battery stability, especially in the first few cycles.

Supporting Information

Supporting Information is available from the Wiley Online Library or from the author.

Acknowledgements

Conflict of Interest

The authors declare no conflict of interest.

Keywords

[1] X. Li, X. Wang, L. Ma, W. Huang, *Adv. Energy Mater.* **2022**, *12*, 2202068.

[2] J. Zhao, J. Zhang, W. Yang, B. Chen, Z. Zhao, H. Qiu, S. Dong, X. Zhou, G. Cui, L. Chen, *Nano Energy* **2019**, *57*, 625.

[3] S. Zhu, Y. Dai, J. Li, C. Ye, W. Zhou, R. Yu, X. Liao, J. Li, W. Zhang, W. Zong, *Sci. Bull.* **2022**, *67*, 1882.

[4] a) K. Ouyang, D. Ma, N. Zhao, Y. Wang, M. Yang, H. Mi, L. Sun, C. He, P. Zhang, *Adv. Funct. Mater.* **2021**, *32*, 2109749; b) L. Cao, D. Li, T. Pollard, T. Deng, B. Zhang, C. Yang, L. Chen, J. Vatamanu, E. Hu, M. J. Hourwitz, L. Ma, M. Ding, Q. Li, S. Hou, K. Gaskell, J. T. Fourkas, X. Q. Yang, K. Xu, O. Borodin, C. Wang, *Nat. Nanotechnol.* **2021**, *16*, 902; c) Y. Huang, Q. Gu, Z. Guo, W. Liu, Z. Chang, Y. Liu, F. Kang, L. Dong, C. Xu, *Energy Storage Mater.* **2022**, *46*, 243.

[5] Z. Liu, J. Ren, F. Wang, X. Liu, Q. Zhang, J. Liu, P. Kaghazchi, D. Ma, Z. Chi, L. Wang, *ACS Appl. Mater. Interf.* **2021**, *13*, 27085.

[6] a) Z. Liu, T. Cui, G. Pulletikurthi, A. Lahiri, T. Carstens, M. Olschewski, F. Endres, *Angew Chem Int Ed Engl* **2016**, *55*, 2889; b) G. Chang, S. Liu, Y. Fu, X. Hao, W. Jin, X. Ji, J. Hu, *Adv. Mater. Interf.* **2019**, *6*, 1901358.

[7] a) R. Yao, L. Qian, Y. Sui, G. Zhao, R. Guo, S. Hu, P. Liu, H. Zhu, F. Wang, C. Zhi, C. Yang, *Adv. Energy Mater.* **2022**, *12*, 2102780; b) Y. Li, P. Wu, W. Zhong, C. Xie, Y. Xie, Q. Zhang, D. Sun, Y. Tang, H. Wang, *Energy Environ. Sci.* **2021**, *14*, 5563; c) Z. Hu, F. Zhang, Y. Zhao, H. Wang, Y. Huang, F. Wu, R. Chen, L. Li, *Adv. Mater.* **2022**, *34*, 2203104.

[8] R. Zhao, H. Wang, H. Du, Y. Yang, Z. Gao, L. Qie, Y. Huang, *Nat. Commun.* **2022**, *13*, 3252.

[9] Z. Wang, M. Zhou, L. Qin, M. Chen, Z. Chen, S. Guo, L. Wang, G. Fang, S. Liang, *eScience* **2022**, *2*, 209.

[10] a) Q. Zhang, Y. Ma, Y. Lu, L. Li, F. Wan, K. Zhang, J. Chen, *Nat. Commun.* **2020**, *11*, 4463; b) Z. Liu, Y. Yang, S. Liang, B. Lu, J. Zhou, *Small Struct.* **2021**, *2*, 2100119.

[11] a) K. Wang, F. Liu, Q. Li, J. Zhu, T. Qiu, X.-X. Liu, X. Sun, *Chem. Eng. J.* **2023**, *452*, 139577; b) T. C. Li, Y. Lim, X. L. Li, S. Luo, C. Lin, D. Fang, S. Xia, Y. Wang, H. Y. Yang, *Adv. Energy Mater.* **2022**, *12*, 2270060.

[12] Y. Dong, S. Di, F. Zhang, X. Bian, Y. Wang, J. Xu, L. Wang, F. Cheng, N. Zhang, *J. Mater. Chem. A* **2020**, *8*, 3252.

[13] H. Li, S. Guo, H. Zhou, *Energy Storage Mater.* **2023**, *56*, 227.

[14] Q. Yang, Q. Li, Z. Liu, D. Wang, Y. Guo, X. Li, Y. Tang, H. Li, B. Dong, C. Zhi, *Adv. Mater.* **2020**, *32*, 2001854.

[15] a) X. Guo, Z. Zhang, J. Li, N. Luo, G.-L. Chai, T. S. Miller, F. Lai, P. Shearing, D. J. L. Brett, D. Han, Z. Weng, G. He, I. P. Parkin, *ACS Energy Lett.* **2021**, *6*, 395; b) D. Han, Z. Wang, H. Lu, H. Li, C. Cui, Z. Zhang, R. Sun, C. Geng, Q. Liang, X. Guo, Y. Mo, X. Zhi, F. Kang, Z. Weng, Q. H. Yang, *Adv. Energy Mater.* **2022**, *12*, 2102982.

[16] Y. Zhang, L. Zhao, Y. Liang, X. Wang, Y. Yao, *eScience* **2022**, *2*, 110.

[17] a) C. Li, X. Zhang, W. He, G. Xu, R. Sun, *J. Power Sources* **2020**, *449*, 227596; b) M. Zhang, R. Liang, T. Or, Y.-P. Deng, A. Yu, Z. Chen, *Small Struct.* **2020**, *2*, 2000064.

[18] G. Li, L. Sun, S. Zhang, C. Zhang, H. Jin, K. Davey, G. Liang, S. Liu, J. Mao, Z. Guo, *Adv. Funct. Mater.* **2023**, 2301291.

[19] R. Qin, S. Ding, C. Hou, L. Liu, Y. Wang, W. Zhao, L. Yao, Y. Shao, R. Zou, Q. Zhao, *Adv. Energy Mater.* **2023**, *13*, 2203915.

[20] a) M. Chuai, J. Yang, M. Wang, Y. Yuan, Z. Liu, Y. Xu, Y. Yin, J. Sun, X. Zheng, N. Chen, W. Chen, *eScience* **2021**, *1*, 178; b) P. Ruan, S. Liang, B. Lu, H. J. Fan, J. Zhou, *Angew. Chem.* **2022**, *134*, e202200598.

[21] a) J. S. Ko, P. P. Paul, G. Wan, N. Seitzman, R. H. DeBlock, B. S. Dunn, M. F. Toney, J. N. Weker, *Chem. Mater.* **2020**, *32*, 3028; b) S. Zhao, C. Li, X. Zhang, N. Li, T. Wang, X. Li, C. Wang, G. Qu, X. Xu, *Kexue Tongbao (Foreign Lang. Ed.)* **2023**, *68*, 56.

[22] L. Ma, S. Chen, H. Li, Z. Ruan, Z. Tang, Z. Liu, Z. Wang, Y. Huang, Z. Pei, J. A. Zapien, C. Zhi, *Energy Environ. Sci.* **2018**, *11*, 2521.

[23] D. Chen, M. Lu, D. Cai, H. Yang, W. Han, *J. Energy Chem.* **2021**, *54*, 712.

[24] G. Liang, F. Mo, X. Ji, C. Zhi, *Nat. Rev. Mater.* **2021**, *6*, 109.

[25] a) Y. Lyu, J. A. Yuwono, P. Wang, Y. Wang, F. Yang, S. Liu, S. Zhang, B. Wang, K. Davey, J. Mao, Z. Guo, *Angew Chem Int Ed Engl* **2023**, *62*, 202303011; b) S. Chen, Y. Ying, S. Wang, L. Ma, H. Huang, X. Wang, X. Jin, S. Bai, C. Zhi, *Angew Chem Int Ed Engl* **2023**, *62*, 202301467.

[26] a) T. Sun, H. J. Fan, *Curr. Opin. Electrochem.* **2021**, *30*, 100799; b) P. Poizot, J. Gaubicher, S. Renault, L. Dubois, Y. Liang, Y. Yao, *Chem. Rev.* **2020**, *120*, 6490; c) Z. Tie, L. Liu, S. Deng, D. Zhao, Z. Niu, *Angew Chem Int Ed Engl* **2020**, *59*, 4920.

[27] J. Xiao, Q. Li, Y. Bi, M. Cai, B. Dunn, T. Glossmann, J. Liu, T. Osaka, R. Sugiura, B. Wu, J. Yang, J.-G. Zhang, M. S. Whittingham, *Nat. Energy* **2020**, *5*, 561.

[28] Z. Wu, J. Zou, Y. Li, E. J. Hansen, D. Sun, H. Wang, L. Wang, J. Liu, *Small* **2022**, *19*, 2206634.

[29] N. Guo, W. Huo, X. Dong, Z. Sun, Y. Lu, X. Wu, L. Dai, L. Wang, H. Lin, H. Liu, H. Liang, Z. He, Q. Zhang, *Small Methods* **2022**, *6*, 2200597.

[30] W. Wang, X. Wei, D. Choi, X. Lu, G. Yang, C. Sun, in *Advances in Batteries for Medium and Large-Scale Energy Storage*, Woodhead Publishing, Sawtson, UK **2015**, 3.

[31] W. Zhang, G. He, *Angew Chem Int Ed Engl* **2023**, *62*, 202218466.

[32] Y. Li, B. Liu, J. Ding, X. Han, Y. Deng, T. Wu, K. Amine, W. Hu, C. Zhong, J. Lu, *Batteries Supercaps* **2020**, *4*, 60.

[33] Y. Wang, T. Wang, S. Bu, J. Zhu, Y. Wang, R. Zhang, H. Hong, W. Zhang, J. Fan, C. Zhi, *Nat. Commun.* **2023**, *14*, 1828.

[34] Z. Lin, T. Liu, X. Ai, C. Liang, *Nat. Commun.* **2018**, *9*, 5262.

[35] R. Weber, M. Genovese, A. Louli, S. Hames, C. Martin, I. G. Hill, J. Dahn, *Nat. Energy* **2019**, *4*, 683.

[36] H. Li, *Joule* **2019**, *3*, 911.

[37] F. He, W. Tang, X. Zhang, L. Deng, J. Luo, *Adv. Mater.* **2021**, *33*, 2105329.

[38] a) M. R. Avila-Costa, T. I. Fortoul, G. Niño-Cabrera, L. Colín-Barenque, P. Bizarro-Nevares, A. L. Gutiérrez-Valdez, J. L. Ordóñez-Librado, V. Rodríguez-Lara, P. Mussali-Galante, P. Díaz-Bech, *Neurotoxicology* **2006**, *27*, 1007; b) S. Ivanković, S. Musić, M. Gotić, N. Ljubešić, *Toxicol. In Vitro* **2006**, *20*, 286.

[39] R. X. S. Tulcan, W. Ouyang, C. Lin, M. He, B. Wang, *Water Res.* **2021**, *207*, 117838.

[40] B. D. Adams, J. Zheng, X. Ren, W. Xu, J. G. Zhang, *Adv. Energy Mater.* **2018**, *8*, 1702097.

[41] L. Ma, M. A. Schroeder, O. Borodin, T. P. Pollard, M. S. Ding, C. Wang, K. Xu, *Nat. Energy* **2020**, *5*, 743.

[42] L. Ma, M. A. Schroeder, T. P. Pollard, O. Borodin, M. S. Ding, R. Sun, L. Cao, J. Ho, D. R. Baker, C. Wang, K. Xu, *Energ. Environm. Mater.* **2020**, *3*, 516.

[43] Z. Chen, J. Zhao, Q. He, M. Li, S. Feng, Y. Wang, D. Yuan, J. Chen, H. N. Alshareef, Y. Ma, *ACS Energy Lett.* **2022**, *7*, 3564.

[44] J. Yu, C. Yu, W. Guo, Z. Wang, Y. Ding, Y. Xie, K. Liu, H. Wang, X. Tan, H. Huang, J. Qiu, *Adv. Funct. Mater.* **2022**, *32*, 2204609.

[45] J. Zheng, T. Tang, Q. Zhao, X. Liu, Y. Deng, L. A. Archer, *ACS Energy Lett.* **2019**, *4*, 1349.

[46] J. Zheng, Y. Deng, W. Li, J. Yin, P. J. West, T. Tang, X. Tong, D. C. Bock, S. Jin, Q. Zhao, *Sci. Adv.* **2022**, *8*, eabq6321.

[47] H. Qiu, X. Du, J. Zhao, Y. Wang, J. Ju, Z. Chen, Z. Hu, D. Yan, X. Zhou, G. Cui, *Nat. Commun.* **2019**, *10*, 5374.

[48] J. H. Park, M. J. Kwak, C. Hwang, K. N. Kang, N. Liu, J. H. Jang, B. A. Grzybowski, *Adv. Mater.* **2021**, *33*, 2101726.

[49] H. Meng, Q. Ran, T. Y. Dai, H. Shi, S. P. Zeng, Y. F. Zhu, Z. Wen, W. Zhang, X. Y. Lang, W. T. Zheng, Q. Jiang, *Nanomicro Lett* **2022**, *14*, 128.

[50] X. Song, H. He, M. H. Aboonasr Shiraz, H. Zhu, A. Khosrozadeh, J. Liu, *Chem Commun (Camb)* **2021**, *57*, 1246.

[51] Q. Ni, H. Jiang, S. Sandstrom, Y. Bai, H. Ren, X. Wu, Q. Guo, D. Yu, C. Wu, X. Ji, *Adv. Funct. Mater.* **2020**, *30*, 2003511.

[52] T. Chen, Y. Wang, Y. Yang, F. Huang, M. Zhu, B. T. W. Ang, J. M. Xue, *Adv. Funct. Mater.* **2021**, *31*, 2101607.

[53] J. Shi, K. Xia, L. Liu, C. Liu, Q. Zhang, L. Li, X. Zhou, J. Liang, Z. Tao, *Electrochim. Acta* **2020**, *358*, 136937.

[54] J. Wang, Q. Zhu, F. Li, J. Chen, H. Yuan, Y. Li, P. Hu, M. S. Kurbanov, H. Wang, *Chem. Eng. J.* **2022**, *433*, 134589.

[55] S. Di, X. Nie, G. Ma, W. Yuan, Y. Wang, Y. Liu, S. Shen, N. Zhang, *Energy Storage Mater.* **2021**, *43*, 375.

[56] Z. Qi, T. Xiong, T. Chen, C. Yu, M. Zhang, Y. Yang, Z. Deng, H. Xiao, W. S. V. Lee, J. Xue, *ACS Appl. Mater. Interf.* **2021**, *13*, 28129.

[57] H. He, J. Liu, *J. Mater. Chem. A* **2020**, *8*, 22100.

[58] X. Zhao, X. Zhang, N. Dong, M. Yan, F. Zhang, K. Mochizuki, H. Pan, *Small* **2022**, *18*, 2200742.

[59] L. Cao, D. Li, T. Deng, Q. Li, C. Wang, *Angew Chem Int Ed Engl* **2020**, *59*, 19292.

[60] N. Zhang, Y. Dong, Y. Wang, Y. Wang, J. Li, J. Xu, Y. Liu, L. Jiao, F. Cheng, *ACS Appl. Mater. Interf.* **2019**, *11*, 32978.

[61] N. Patil, C. de la Cruz, D. Ciurduc, A. Mavrandonakis, J. Palma, R. Marcilla, *Adv. Energy Mater.* **2021**, *11*, 2100939.

[62] L. Ma, J. Z. Lee, T. P. Pollard, M. A. Schroeder, M. A. Limpert, B. Craven, S. Fess, C. S. Rustomji, C. S. Wang, O. Borodin, K. Xu, *ACS Energy Lett.* **2021**, *6*, 4426.

[63] L. Ma, S. Chen, N. Li, Z. Liu, Z. Tang, J. A. Zapien, S. Chen, J. Fan, C. Zhi, *Adv. Mater.* **2020**, *32*, 1908121.

[64] A. Chen, C. Zhao, Z. Guo, X. Lu, J. Zhang, N. Liu, Y. Zhang, N. Zhang, *Adv. Funct. Mater.* **2022**, *32*, 2203595.

[65] J. Hao, X. Li, S. Zhang, F. Yang, X. Zeng, S. Zhang, G. Bo, C. Wang, Z. Guo, *Adv. Funct. Mater.* **2020**, *30*, 2001263.

2300660 (14 of 16)

**ADVANCED
SCIENCE NEWS**

www.advancedsciencenews.com

**small
methods**

www.small-methods.com

[66] Y. Shang, P. Kumar, U. Mittal, X. Liang, D. Kundu, *Energy Stor. Mater.* **2023**, *55*, 117.

[67] L. T. Hieu, S. So, I. T. Kim, J. Hur, *Chem. Eng. J.* **2021**, *411*, 128584.

[68] Y. Mu, T. Zhou, D. Li, W. Liu, P. Jiang, L. Chen, H. Zhou, G. Ge, *Chem. Eng. J.* **2022**, *430*, 132839.

[69] J. Yang, R. Zhao, Y. Wang, Y. Bai, C. Wu, *Energy Material Advances* **2022**, *2022*, 9809626.

[70] N. Chang, T. Li, R. Li, S. Wang, Y. Yin, H. Zhang, X. Li, *Energy Environ. Sci.* **2020**, *13*, 3527.

[71] Y. An, Y. Tian, K. Zhang, Y. Liu, C. Liu, S. Xiong, J. Feng, Y. Qian, *Adv. Funct. Mater.* **2021**, *31*, 2101886.

[72] C. Wu, C. Sun, K. Ren, F. Yang, Y. Du, X. Gu, Q. Wang, C. Lai, *Chem. Eng. J.* **2023**, *452*, 139465.

[73] M. Zhou, S. Guo, J. Li, X. Luo, Z. Liu, T. Zhang, X. Cao, M. Long, B. Lu, A. Pan, *Adv. Mater.* **2021**, *33*, 2100187.

[74] S. Cora, S. Ahmad, N. Sa, *ACS Appl. Mater. Interf.* **2021**, *13*, 10131.

[75] C. Xiao, R. Yao, H. Zhu, L. Qian, C. Yang, *Chem. Commun.* **2022**, *58*, 10088.

[76] L. Cao, D. Li, F. A. Soto, V. Ponce, B. Zhang, L. Ma, T. Deng, J. M. Seminario, E. Hu, X. Q. Yang, P. B. Balbuena, C. Wang, *Angew Chem Int Ed Engl* **2021**, *60*, 18845.

[77] C. Zhang, J. Holoubek, X. Wu, A. Daniyar, L. Zhu, C. Chen, D. P. Leonard, I. A. Rodriguez-Perez, J. X. Jiang, C. Fang, X. Ji, *Chem Commun (Camb)* **2018**, *54*, 14097.

[78] X. Ji, *eScience* **2021**, *1*, 99.

[79] Q. Zhang, Y. Ma, Y. Lu, L. Li, F. Wan, K. Zhang, J. Chen, *Nat. Commun.* **2020**, *11*, 4463.

[80] C. Zhang, W. Shin, L. Zhu, C. Chen, J. C. Neuefeind, Y. Xu, S. I. Allec, C. Liu, Z. Wei, A. Daniyar, J. X. Jiang, C. Fang, P. Alex Greaney, X. Ji, *Carbon Energy* **2020**, *3*, 339.

[81] L. Qian, W. Yao, R. Yao, Y. Sui, H. Zhu, F. Wang, J. Zhao, C. Zhi, C. Yang, *Adv. Funct. Mater.* **2021**, *31*, 2105736.

[82] L. Wang, Y. Zhang, H. Hu, H.-Y. Shi, Y. Song, D. Guo, X.-X. Liu, X. Sun, *ACS Appl. Mater. Interfaces* **2019**, *11*, 42000.

[83] P. Lin, J. Cong, J. Li, M. Zhang, P. Lai, J. Zeng, Y. Yang, J. Zhao, *Energy Storage Mater.* **2022**, *49*, 172.

[84] J. Cong, X. Shen, Z. Wen, X. Wang, L. Peng, J. Zeng, J. Zhao, *Energy Storage Mater.* **2021**, *35*, 586.

[85] D. Chao, W. Zhou, C. Ye, Q. Zhang, Y. Chen, L. Gu, K. Davey, S. Z. Qiao, *Angew Chem Int Ed Engl* **2019**, *58*, 7823.

[86] C. Gao, J. Wang, Y. Huang, Z. Li, J. Zhang, H. Kuang, S. Chen, Z. Nie, S. Huang, W. Li, Y. Li, S. Jin, Y. Pan, T. Long, J. Luo, H. Zhou, X. Wang, *Nanoscale* **2021**, *13*, 10100.

[87] Q. Jian, Y. Wan, Y. Lin, M. Ni, M. Wu, T. Zhao, *ACS Appl. Mater. Interfaces* **2021**, *13*, 52659.

[88] K. Zhao, C. Wang, Y. Yu, M. Yan, Q. Wei, P. He, Y. Dong, Z. Zhang, X. Wang, L. Mai, *Adv. Mater. Interf.* **2018**, *5*, 1800848.

[89] D. Kundu, B. D. Adams, V. Duffort, S. H. Vajargah, L. F. Nazar, *Nat. Energy* **2016**, *1*, 16119.

[90] Y. Dong, M. Jia, Y. Wang, J. Xu, Y. Liu, L. Jiao, N. Zhang, *ACS Appl. Energy Mater.* **2020**, *3*, 11183.

[91] Y. Wu, Z. Zhu, D. Shen, L. Chen, T. Song, T. Kang, Z. Tong, Y. Tang, H. Wang, C. S. Lee, *Energy Storage Mater.* **2021**, *45*, 1084.

[92] Y. Zhu, J. Yin, X. Zheng, A.-H. Emwas, Y. Lei, O. F. Mohammed, Y. Cui, H. N. Alshareef, *Energy Environ. Sci.* **2021**, *14*, 4463.

[93] D. Bin, W. Huo, Y. Yuan, J. Huang, Y. Liu, Y. Zhang, F. Dong, Y. Wang, Y. Xia, *Chem* **2020**, *6*, 968.

[94] N. Zhang, M. Jia, Y. Dong, Y. Wang, J. Xu, Y. Liu, L. Jiao, F. Cheng, *Adv. Funct. Mater.* **2019**, *29*, 1807331.

[95] F. Wang, L. E. Blanc, Q. Li, A. Faraone, X. Ji, H. H. Chen-Mayer, R. L. Paul, J. A. Dura, E. Hu, K. Xu, L. F. Nazar, C. Wang, *Adv. Energy Mater.* **2021**, *11*, 2102016.

[96] X. Feng, J. Zhai, L. Jiang, *Angew Chem Int Ed Engl* **2005**, *44*, 5115.

[97] T. Chen, Y. Wang, Y. Yang, F. Huang, M. Zhu, B. T. W. Ang, J. M. Xue, *Adv. Funct. Mater.* **2021**, *31*, 2101607.

[98] Z. Zhang, S. Said, K. Smith, Y. S. Zhang, G. He, R. Jervis, P. R. Shearing, T. S. Miller, D. J. L. Brett, *J. Mater. Chem. A* **2021**, *9*, 15355.

[99] C. Ma, A. Nikiforov, D. Hegemann, N. De Geyter, R. Morent, K. Ostrikov, *Int. Mater. Rev.* **2023**, *68*, 82.

[100] W. Du, S. Huang, Y. Zhang, M. Ye, C. C. Li, *Energy Storage Mater.* **2022**, *45*, 465.

[101] B. Liu, S. Wang, Z. Wang, H. Lei, Z. Chen, W. Mai, *Small* **2020**, *16*, 2001323.

[102] C. Yuan, L. Yin, P. Du, Y. Yu, K. Zhang, X. Ren, X. Zhan, S. Gao, *Chem. Eng. J.* **2022**, *442*, 136231.

[103] W. Pfleging, *Int. J. Extreme Manuf.* **2020**, *3*, 012002.

[104] H. Lu, Q. Jin, X. Jiang, Z. M. Dang, D. Zhang, Y. Jin, *Small* **2022**, *18*, e2200131.

[105] J. Zheng, Q. Zhao, T. Tang, J. Yin, C. D. Quilty, G. D. Renderos, X. Liu, Y. Deng, L. Wang, D. C. Bock, *Science* **2019**, *366*, 645.

[106] a) X. Chen, W. Li, S. Hu, N. G. Akhmedov, D. Reed, X. Li, X. Liu, *Nano Energy* **2022**, *98*, 107269; b) C. Huang, W. Deng, X. Yuan, Y. Zhou, C. Li, J. Hu, M. Zhang, J. Zhu, R. Li, *ACS Appl. Mater. Interf.* **2022**, *15*, 2341.

[107] a) H. He, H. Tong, X. Song, X. Song, J. Liu, *J. Mater. Chem. A* **2020**, *8*, 7836; b) Z. Zeng, Z. Zeng, L. Sun, H. Mi, L. Deng, P. Zhang, X. Ren, Y. Li, *Nanoscale* **2021**, *13*, 12223.

[108] J. Zheng, Z. Cao, F. Ming, H. Liang, Z. Qi, W. Liu, C. Xia, C. Chen, L. Cavallo, Z. Wang, H. N. Alshareef, *ACS Energy Lett.* **2021**, *7*, 197.

[109] H. Zhao, Q. Fu, X. Luo, X. Wu, S. Indris, M. Bauer, Y. Wang, H. Ehrenberg, M. Knapp, Y. Wei, *Energy Storage Mater.* **2022**, *50*, 464.

[110] M. Qiu, P. Sun, A. Qin, G. Cui, W. Mai, *Energy Storage Mater.* **2022**, *49*, 463.

[111] a) S. Chen, C. Niu, H. Lee, Q. Li, L. Yu, W. Xu, J.-G. Zhang, E. J. Dufek, M. S. Whittingham, S. Meng, J. Xiao, J. Liu, *Joule* **2019**, *3*, 1094; b) L. Wang, Z. Wu, J. Zou, P. Gao, X. Niu, H. Li, L. Chen, *Joule* **2019**, *3*, 2086.

[112] H. Yang, T. Zhang, D. Chen, Y. Tan, W. Zhou, L. Li, W. Li, G. Li, W. Han, H. J. Fan, *Adv. Mater.* **2023**, *35*, 2300053.

[113] Y. Zhang, Z. Chen, H. Qiu, W. Yang, Z. Zhao, J. Zhao, G. Cui, *NPG Asia Mater.* **2020**, *12*, 4.

[114] Y. Fang, X. Xie, B. Zhang, Y. Chai, B. Lu, M. Liu, J. Zhou, S. Liang, *Adv. Funct. Mater.* **2021**, *32*, 2109671.

[115] M. Ghosh, V. Vijayakumar, B. Anothumakkool, S. Kurungot, *ACS Sustainable Chem. Eng.* **2020**, *8*, 5040.

[116] Z. Chang, H. Yang, A. Pan, P. He, H. Zhou, *Nat. Commun.* **2022**, *13*, 6788.

[117] Y. Ma, J. Wan, Y. Yang, Y. Ye, X. Xiao, D. T. Boyle, W. Burke, Z. Huang, H. Chen, Y. Cui, Z. Yu, S. T. Oyakhire, Y. Cui, *Adv. Energy Mater.* **2022**, *12*, 2103720.

[118] G. Zampardi, F. L. Mantia, *Nat. Commun.* **2022**, *13*, 687.

[119] H. Hesse, M. Schimpe, D. Kucevic, A. Jossen, *Energies* **2017**, *10*, 2107.

[120] Y. Liang, C. Z. Zhao, H. Yuan, Y. Chen, W. Zhang, J. Q. Huang, D. Yu, Y. Liu, M. M. Titirici, Y. L. Chueh, H. Yu, Q. Zhang, *InfoMat* **2019**, *1*, 6.

[121] M. Tao, Y. Xiang, D. Zhao, P. Shan, Y. Yang, *Communicat. Mater.* **2022**, *3*, 50.
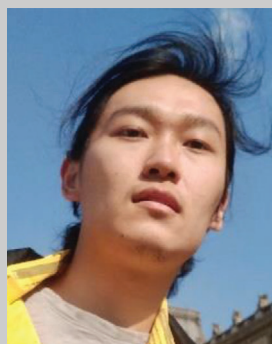
Zhenrui Wu is a Ph.D. candidate at the University of British Columbia (UBC), Canada. Zhenrui earned his MA.Sc. in mechanical engineering from UBC in 2019. His primary research focuses on "Beyond-Li" batteries, with a previous emphasis on K-ion batteries. Zhenrui's research has now transitioned toward the nuanced aspects of zinc-electrolyte and cathode-electrolyte interfaces in Zn-ion batteries, placing a particular emphasis on understanding the effects of electrolytes and conducting an in-depth analysis of gaseous byproducts.

Yihu Li is currently pursuing his Ph.D. at Chalmers University of Technology. He obtained his Master's degree from Central South University, where he delved into electrolyte optimization for aqueous zinc ion batteries. His evolving research pursuits now center on sodium batteries, specifically focusing on designing electrolytes and investigating interfaces.

Jian Liu is an associate professor in the School of Engineering at the University of British Columbia (UBC) Okanagan campus, Canada. Dr. Liu received his Ph.D. in materials science (2013) from the University of Western Ontario (Canada) and worked as an NSERC postdoctoral fellow at Lawrence Berkeley National Laboratory and Pacific Northwest National Laboratory before joining UBC in January 2017. His current research interests focus on advanced nanofabrication techniques, materials design for Li-ion batteries and beyond, and interfacial control and understanding in energy storage and conversion systems.